

This discussion paper is/has been under review for the journal Solid Earth (SE).  
Please refer to the corresponding final paper in SE if available.

# Evolution of a highly dilatant fault zone in the grabens of Canyonlands National Park, Utah/USA – integrating field work, ground penetrating radar and airborne imagery analysis

M. Kettermann<sup>1</sup>, C. Grützner<sup>2,\*</sup>, H. W. van Gent<sup>1,\*\*</sup>, J. L. Urai<sup>1</sup>, K. Reicherter<sup>2</sup>, and J. Mertens<sup>1,\*\*\*</sup>

<sup>1</sup>Structural Geology, Tectonics and Geomechanics Energy and Mineral Resources Group, RWTH Aachen University, Lochnerstraße 4–20, 52056 Aachen, Germany

<sup>2</sup>Neotectonics and Natural Hazards, RWTH Aachen University, Lochnerstraße 4-20, 52056 Aachen, Germany

\* now at: Bullard Laboratories, Department of Earth Sciences, University of Cambridge, Cambridge, UK

\*\* now at: Shell Global Solutions International, Rijswijk, the Netherlands

\*\*\* now at: ETH Zürich, Zürich, Switzerland

## Evolution of a highly dilatant fault zone in the grabens of Canyonlands National Park

M. Kettermann et al.

Title Page

Abstract

Introduction

Conclusions

References

Tables

Figures

◀

▶

◀

▶

Back

Close

Full Screen / Esc

Printer-friendly Version

Interactive Discussion

Received: 20 February 2015 – Accepted: 23 February 2015 – Published: 17 March 2015

Correspondence to: M. Kettermann (michael.kettermann@emr.rwth-aachen.de)

Published by Copernicus Publications on behalf of the European Geosciences Union.

**SED**

7, 1119–1161, 2015

**Evolution of a highly dilatant fault zone in the grabens of Canyonlands National Park**

M. Kettermann et al.

Title Page

Abstract

Introduction

Conclusions

References

Tables

Figures



Back

Close

Full Screen / Esc

Printer-friendly Version

Interactive Discussion



## Abstract

The grabens of the Canyonlands National Park are a young and active system of sub-parallel, arcuate grabens, whose evolution is the result of salt movement in the subsurface and a slight regional tilt of the faulted strata. We present results of ground penetrating radar surveys in combination with field observations and analysis of high resolution airborne imagery. GPR data show intense faulting of the Quaternary sediments at the flat graben floors, implying a more complex fault structure than visible at the surface. Direct measurements of heave and throw at several locations to infer fault dips at depth, combined with observations of primary joint surfaces in the upper 100 m suggest a model of the highly dilatant fault geometry in profile. Sinkholes observed in the field as well as in airborne imagery give insights in local massive dilatancy and show where water and sediments are transported underground. Based on correlations of paleosols observed in outcrops and GPR profiles, we argue that the grabens in Canyonlands National Park are either older than previously assumed, or that sedimentation rates were much higher in the Pleistocene.

## 1 Introduction

Understanding the structure of dilatant fractures in normal fault zones is important for many applications in geoscience. Reservoirs for hydrocarbons, geothermal energy and fresh water often contain dilatant fractures (e.g. Ehrenberg and Nadeau, 2005; Wennberg et al., 2008; Jafari and Babadagli, 2011). A better understanding of the internal structures of such fault zones is required to extrapolate fault geometries in typical reservoir depths below the industrial seismic resolution. This is especially complicated when failure structures of different generations produce a mechanical stratigraphy and ultimately interact with each other.

In this paper we present a case study focusing on the spectacular grabens of the Needles Fault Zone in Canyonlands National Park, Utah, USA (field photographs

## SED

7, 1119–1161, 2015

### Evolution of a highly dilatant fault zone in the grabens of Canyonlands National Park

M. Kettermann et al.

Title Page

Abstract

Introduction

Conclusions

References

Tables

Figures

◀

▶

◀

▶

Back

Close

Full Screen / Esc

Printer-friendly Version

Interactive Discussion



## Evolution of a highly dilatant fault zone in the grabens of Canyonlands National Park

M. Kettermann et al.

Title Page

Abstract

Introduction

Conclusions

References

Tables

Figures

◀

▶

◀

▶

Back

Close

Full Screen / Esc

Printer-friendly Version

Interactive Discussion

Fig. 1a–c), a fault array that reactivates two pre-existing major joint sets. The area is well known as reservoir analogue, and sedimentary rocks and soil are well exposed due to the semi-arid climate. Estimates of the beginning of graben formation vary from 60–80 ka (based on the dating of sediments in deep open fissures (Biggar and Adams, 1987) to 1.4 Ma, which is the estimated time of incision of the Colorado River (Schultz-Ela and Walsh, 2002). Present day motions are known from interpretation of InSAR data (Furuya et al., 2007). Reheis et al. (2005) were able to date Quaternary strata deposited during active formation of the grabens. These studies show that the grabens of the Canyonlands are an active fault zone with syntectonic sedimentation. The goal of this study is to better understand the coupling between deformation, erosion and deposition in such an active system, as well as a to gain insights on the internal structure of dilatant fracture systems. To this end, we combine detailed field analyses with ground penetrating radar and remote sensing data.

## 2 The Needles Fault Zone

The Needles Fault Zone is located in Canyonlands National Park on the western rim of the Paradox Basin in southeastern Utah/USA (Fig. 2). This zone of extensive faulting is characterized by an arcuate array of grabens, also known as *the Grabens*, that extends over 20 km southward from the Colorado and Green River confluence and 5–6 km eastwards from the Colorado River. The grabens strike NNE–SSW in the northern section and gradually change to a more E–W orientation in the southern section (Fig. 3b; e.g. McGill and Stromquist, 1979). The most spectacular grabens are the northern ones, named (from east to west) Devil’s Pocket, Devil’s Lane, Cyclone Canyon, Red Lake Canyon, Twin Canyon and Lens Canyon. Grabens were proposed to become younger further to the east (Huntoon, 1982).

The regional tectonic influence of the Monument Upwarp (Fig. 2), a regional fold structure developed during the Laramide Orogeny in early Tertiary (Golstrand, 1994; Condon, 1997; Walsh and Schultz-Ela, 2003), caused differential local tilting of the

Needles Fault Zone, ranging from 2° toward NW (Walsh and Schultz-Ela, 2003; Furuya et al., 2007) to 4° toward WNW (McGill and Stromquist, 1979; Huntoon, 1982; Trudgill and Cartwright, 1994).

The stratigraphy of the study area consists of more than 300 m of Pennsylvanian evaporites at the base, mainly halite, gypsum and anhydrite (e.g. Cartwright et al., 1995). These units are nowadays located at depths between 300 and 500 m, and crop out only within the Colorado River incision (e.g. Mertens, 2006). These are overlain by sandstones, intercalated shales and limestones of the Pennsylvanian, and the prominently jointed Permian Cedar Mesa sandstones on top (Lewis and Campbell, 1965; Huntoon, 1982; McGill et al., 2000). This entire overlying sediment package reaches up to 500 m in thickness (e.g. McGill and Stromquist, 1979; Trudgill and Cartwright, 1994; Schultz and Moore, 1996; Cartwright and Mansfield, 1998; Moore and Schultz, 1999; Fossen et al., 2010).

At the present day the Grabens are filled with unconsolidated Quaternary soft sediments. According to the geological map of Billingsley et al. (2002) most of Devil's Pocket, and Cyclone Canyon as well as northern Devil's Lane are dominated by Holocene and Pleistocene alluvial deposits. The southern section of Devil's Lane is mostly filled with Holocene alluvial fan deposits. Isolated depressions permitted ponding of Holocene silt and mud in Devil's Lane and Cyclone Canyon with sediment thicknesses up to two meters. Faulting significantly influences distribution of local deposition centers and the drainage system (Trudgill, 2002). All grabens show occasional rock fall debris.

Incision of the Colorado River, in combination with the local tilt is seen by most researchers as cause for the formation of the grabens, either due to salt movement or gravitational gliding. Huntoon (1982) proposed that salt movement occurs as a reaction to the unloading effect of the incising Colorado expressed as the Meander Anticline, a fold structure following the Colorado River with the stream flowing in the fold axis striking roughly NNE. Furuya et al. (2007) showed by using interferometric synthetic aperture radar (InSAR) measurements that the uplift of the Meander Anticline as well

**Evolution of a highly dilatant fault zone in the grabens of Canyonlands National Park**

M. Kettermann et al.

Title Page

Abstract

Introduction

Conclusions

References

Tables

Figures

◀

▶

◀

▶

Back

Close

Full Screen / Esc

Printer-friendly Version

Interactive Discussion

## Evolution of a highly dilatant fault zone in the grabens of Canyonlands National Park

M. Kettermann et al.

Title Page

Abstract

Introduction

Conclusions

References

Tables

Figures

◀

▶

◀

▶

Back

Close

Full Screen / Esc

Printer-friendly Version

Interactive Discussion



as the graben formation is ongoing, which is expressed most prominently by NW oriented extensional movements of up to  $3 \text{ mm a}^{-1}$  in the south of the grabens. Faulting in the Canyonlands National Park occurs as aseismic creep-faulting, the only recorded earthquake activity was a series of microquakes in spring of 1987 with magnitudes  $M_L \leq 1.8$  in depth of 6–10 km, which is below the decoupling salt layer (Wong et al., 1993; Moore and Schultz, 1999).

To investigate sediment thicknesses and their distribution, Grosfils et al. (2003) and Abrahamson (2005) used seismic refraction surveys in northern Devils Lane and Cyclone Canyon, respectively. Grosfils et al. (2003) additionally collected gravity data. Evaluation of the data lets them estimate maximum thicknesses of Pleistocene and Holocene sediments of more than 90 m in Devils Lane and 60–75 m in Cyclone Canyon. The resulting total throw (i.e. sediment thickness plus graben wall height) in both grabens exceeds earlier estimates (e.g. Cartwright et al., 1995) by a factor of up to 1.5 (e.g.  $\geq 145 \text{ m}$  instead of  $\leq 105 \text{ m}$  for the Master fault in Devil's Lane). In the following we distinguish between the terms graben-bounding fault, which is the actual fault plane and fault position forming the graben, and graben wall, which is the exposed rock on either side of the graben. The latter is almost invariably an original joint surface, in many cases affected by weathering.

In the northern section, the upper hundred meters of outcropping hard rock are cut by two characteristic regular joint sets (e.g. McGill and Stromquist, 1979). One joint-set strikes NNE, the second one to SE. Both joint sets change their orientation slightly towards the south, the NNE set following the change of the graben orientation, the second joint set stays roughly normal to the first one with a deviation of up to  $30^\circ$  in the vicinity of eastern Chesler Canyon. According to the considerations of McGill and Stromquist (1979) these latter joints are older than the grabens. Their considerations are based on the variety of different angles between joint strike and graben wall orientation, which are neither consistent with shear nor extensional origin of jointing. Additionally, the observation of joints with regular spacing at exposed graben floors (e.g. northern Devil's Lane) imply that they are older than the graben faults. Several

papers have interpreted that the faults developed in a way strongly influenced by the preexisting joints (McGill and Stromquist, 1979; Cartwright and Mansfield, 1998; McGill et al., 2000; Trudgill, 2002). The effect of joints on the geometry of fault tips has been described by Cartwright and Mansfield (1998), but an extensive analysis of the fault–joint relationship considering faults and joints in the entire grabens area and the related structures has not been done before.

### 3 Data sources and methodology

Detailed mapping of faults and joints as well as a remote sensing analysis of topography and structures was carried out as base for geophysical data collection and field mapping. We used high resolution ( $25\text{ cm pixel}^{-1}$ ) airborne orthoimagery (Utah Automated Geographic Reference Center, 2009) for the northern section and aerial images with 1 m resolution (National Agriculture Imagery Program, 2009) for the southern parts. These images are also used in the figures of this paper.

In addition to remote sensing, classical field mapping with GPS, compass, high-resolution photographs, and a laser rangefinder, we used a ground penetrating radar system by GSSI (Salem, USA) to image subsurface features. The survey equipment consisted of the SIR 3000 field computer with GPS tracker, 100 and 400 MHz antennas, and a survey wheel. We aimed at reaching penetration depths up to 10 m or more with the lower-frequency antenna. Data with a surface-near resolution better than 10 cm are routinely gathered by the 400 MHz system. Data processing was performed with the ReflexW software package (Sandmeier, 2011) and included static corrections, background removal, gain adjustments, and frequency filtering. Topographic correction (Neal, 2004) was applied to those profiles with significant topographic variations only.

Wave travel times were converted into depths based on literature velocity values and hyperbola analyses where possible. Values between  $0.1$  and  $0.15\text{ m ns}^{-1}$  were expected for the relatively dry sandy soils present in the Canyonlands National Park (Smith and Jol, 1995; Heteren et al., 1998). Diffraction hyperbolae that were caused by

SED

7, 1119–1161, 2015

## Evolution of a highly dilatant fault zone in the grabens of Canyonlands National Park

M. Kettermann et al.

Title Page

Abstract

Introduction

Conclusions

References

Tables

Figures

◀

▶

◀

▶

Back

Close

Full Screen / Esc

Printer-friendly Version

Interactive Discussion



single blocks in several profiles revealed velocities of  $0.125 \pm 0.005 \text{ m ns}^{-1}$ . This value was used for the time-depth-conversion in the profiles.

Vertical resolution of the data depends on the wave velocity as well. Maximum achievable vertical resolution is a quarter of the wavelength (wavelength equals wave velocity divided by frequency:  $\lambda = v/f$ ; Neal, 2004), and thus approximately 8 cm for the 400 MHz antenna in our study.

A total of 66 GPR profiles were collected with a cumulative length of more than 7 km, distributed over Devils Pocket, Devils Lane, and Cyclone Canyon. The different antenna types were used to achieve either higher penetration depth or better resolution, respectively. Profiles normal to fault strike were investigated with both antennas as we expect them to show more structures than strike parallel profiles. For minimum invasion on the sensitive biological soil crust (Rosentreter et al., 2007) we restricted our surveys to existing tracks and trails in agreement with the National Park Service.

## 4 Remote sensing

Modern airborne orthorectified photos with very high resolution (up to  $25 \text{ cm pixel}^{-1}$ ) allow a detailed remote mapping of joints and faults in the Needles Fault Zone. To analyze orientations of the joint generations and the fault system we mapped more than 20 000 joints and 800 faults. Figure 4 shows all faults, divided into four sections with similar orientations. For each of the sections we plotted rose diagrams of fault and joint orientations and for each section an airborne photograph is given with interpreted faults (white lines) and joints (red lines) as illustration of our interpretations. Within each section the orientations are quite constant and one joint set is always parallel to the main faults. A detailed map showing joints and faults overlain on aerial photographs is included in the Supplement.

# Evolution of a highly dilatant fault zone in the grabens of Canyonlands National Park

M. Kettermann et al.

Title Page

Abstract

Introduction

Conclusions

References

Tables

Figures

◀

▶

◀

▶

Back

Close

Full Screen / Esc

Printer-friendly Version

Interactive Discussion



## 5 Field observations

We focused on Devil's Pocket, Devil's Lane and Cyclone Canyon because in these grabens the walls are less weathered and jointing is most distinct, but included an excursion to Cross Canyon in the south and Lens Canyon in the west. Besides the GPR data that are described later we also collected basic geometric information of these grabens using a laser range-finder and visual observations. Three major findings are of importance:

1. Along the 4wd track leading from Devils Lane southwards along the Bobby Jo Camp to Bobby's Hole we observed a number of localized depressions at graben boundaries and faults, interpreted as sinkholes in agreement with work by (Biggar and Adams, 1987). The sinkholes can reach from few meters to tens of meters in length and several meters in depth. They were mapped from field observations and orthoimages (for map distribution see Fig. 3). Numerous sinkholes observed in airborne imagery are not located at graben boundaries, but coincide with faults within or across grabens. Figure 5a shows an example of an airborne image of such a sinkhole located at the eastern graben wall in a graben east of Cow Canyon (see arrow "1" in Fig. 3). A channel like structure protruding towards the graben wall indicates sediment transport towards the depression at the graben wall. The corresponding field photograph (Fig. 5b) shows the geometry and extent of this sinkhole. Apparently, water as well as transported sediment disappears underground at these locations. Due to their depth of several meters they often act as a trap for the abundant tumble weed. It is unclear though, whether there is an interconnected system of open fractures that allows a transport of sediments over larger distances, or the opening rate of these fissures is larger than sediment input, so that they do not fill up. Figure 5c shows a sinkhole that is not located at a graben boundary but at a graben-crossing fault (for location see arrow "2" in Fig. 3). The corresponding field photograph (d) shows the dimension of the sinkhole and the void where rainwater and sediments are transported

SED

7, 1119–1161, 2015

### Evolution of a highly dilatant fault zone in the grabens of Canyonlands National Park

M. Kettermann et al.

Title Page

Abstract

Introduction

Conclusions

References

Tables

Figures

◀

▶

◀

▶

Back

Close

Full Screen / Esc

Printer-friendly Version

Interactive Discussion





## 6 GPR observations

A number of profiles selected for their descriptive value are shown and interpreted in the following paragraphs. Especially the profiles crossing from a graben to a horst, thus being crosscuts of a graben-bounding fault, show the most interesting results.

5 The given examples illustrate sediments dipping towards the graben wall, sediments dipping towards the graben center, changing deposition rates within a graben and graben internal faulting. Dip angles of the faults cannot be determined exactly since depth migration of the GPR data was not possible due to amplification of artefacts during migration. The location of all described profiles is illustrated in Fig. 3a with  
10 numbers according to the subheadings.

### 6.1 Devil's Lane WE-profile

The profiles were acquired with both the 400 (Fig. 8b) and 100 (Fig. 8d) MHz antenna and stitched from two segments each (see white suture lines). They cross Devils Lane from the western graben wall over 135 m to ESE as illustrated in Fig. 8a. Our  
15 interpretations are depicted in Fig. 8c and e for the 400 MHz profile and the 100 MHz profile, respectively.

Both antennas image sediments dipping towards the graben bounding fault over a length of 30–40 m, but differing in the depth at which they can be observed. Whereas layers may be interpreted to become horizontal at a depth of around 2.5 m in the  
20 400 MHz profile, the 100 MHz antenna shows dipping structures down to 5 m depth. The discrepancy is assumed to be the result of different resolutions. In the airborne imagery (a) this area coincides with darker colors, indicating more humidity and a slight surface depression, which is also observable in the field.

More localized areas of dipping strata are observed in three other positions. Dips  
25 from the west towards the 60 m mark can be observed in the 400 MHz profile as well as dips from the east towards the 60 m mark, at depths of up to approximately 1.5 m. These are not visible in the 100 MHz profile, although here some dipping occurs

## Evolution of a highly dilatant fault zone in the grabens of Canyonlands National Park

M. Kettermann et al.

Title Page

Abstract

Introduction

Conclusions

References

Tables

Figures

◀

▶

◀

▶

Back

Close

Full Screen / Esc

Printer-friendly Version

Interactive Discussion



## Evolution of a highly dilatant fault zone in the grabens of Canyonlands National Park

M. Kettermann et al.

Title Page

Abstract

Introduction

Conclusions

References

Tables

Figures

◀

▶

◀

▶

Back

Close

Full Screen / Esc

Printer-friendly Version

Interactive Discussion

from 60 m westwards in depths between 2 and 5 m. Some west dipping layers in the upper meter are found in the 400 MHz profile between 85 and 90 m but not at all using 100 MHz. Finally some east dipping strata occur east of 115 m (400 MHz) down to 1 m and east of 125 m (100 MHz) between 2 and 3.5 m depth. In general, both antennas

5 show very similar features at the same positions, although they differ in the depths in which the observations can be made.

In addition to dipping sediments we interpret a number of faults in these profiles, which cannot be seen at the surface (Fig. 8c and e). These faults mostly correlate between both profiles, although some smaller faults seen in the 400 MHz profile could

10 not be resolved in the 100 MHz profile. The average spacing between the faults is about 10–15 m. Many faults reach up close to the surface, but there are also some that show no more offset in several meters depths.

### 6.2 Northern Cyclone Canyon WE-profile

This 100 MHz profile in northern Cyclone Canyon starts at the western graben wall and follows the trail towards SE (see Fig. 9a). It shows a sediment package of about

15 10 m thickness dipping from the surface down to 10–20 m depth over a length of 100 m along the profile. This dip is only an apparent dip, as the actual structure is unknown (e.g. alluvial fan). The overlying horizontal layers gain thickness along the profile and finally reach down to 10 m.

In this profile there are also faults to be found as illustrated by dashed lines and named in Fig. 9c. We interpret three major faults and four associated minor faults. Fault 1 is clearly visible due to terminating reflectors and a change in reflector intensity at the 16 m mark. This fault is interpreted to be the graben bounding fault of the northern graben segment. Faults 2 and 3 are located more distal from the graben-wall and both

20 show small associated faults to their west. Again, terminating reflectors and changes in reflector intensity indicate the existence of these faults. The strike direction of faults 2 and 3 is uncertain, but we assume them to be parallel to fault 1, following the general



## Evolution of a highly dilatant fault zone in the grabens of the Canyonlands National Park

M. Kettermann et al.

Title Page

Abstract

Introduction

Conclusions

References

Tables

Figures

◀

▶

◀

▶

Back

Close

Full Screen / Esc

Printer-friendly Version

Interactive Discussion

and shows at least three fault strands as illustrated by dashed lines in Fig. 11c. Caused by the lack of GPR information, the lower extent of the fault cannot be determined. Nevertheless, all fault strands appear to have their upper fault tip in a depth of about 0.5 m. Fault 2 (at 115 m) is less sharply defined and characterized by reflectors dipping diffusely towards the interpreted slip plane. Its upper termination is again assumed in a depth of 0.5 m. The assumed fault traces for both faults are also marked on the airborne photograph (Fig. 11a) by black dashed lines.

Sedimentary structures vary strongly throughout the profile. The westernmost section has sediments dipping towards fault 1 at a depth of 0.5–2 m, while in the uppermost 0.5 m west dipping layers are overlaying the faulted segment. These west dipping layers extend to a depth of about 3 m on the eastern side of fault 1 and show lateral extends from 20–30 m. Layers in the upper 30–40 cm of the entire profile are horizontal. Sediments at fault 2 dip towards it from both sides but in a rather small lateral extend of about 5–10 m each. At the easternmost section of the profile layers dip to the west in depths of 1–2.5 m and a lateral extend of roughly 25 m. Parts not affected by the described dipping layers are characterized by horizontal reflectors through the entire sediment layer down to 5 m.

## 7 Interpretation and discussion

Combined with the field and remote sensing data (observations, mapping, airborne imagery and digital elevation models), the information derived from the GPR profiles support and enhances the knowledge of how the grabens form and which processes are involved:

### 7.1 Evidence for dilatant faulting

Evidence for dilatant faulting is the occurrence of sinkholes that we observed along graben bounding faults in the more eastern grabens (cf. Fig. 3). Tensile opening gaps

allow water and sediments to be transported underground (Fig. 5). Analysis of airborne imagery showed several sinkholes located within grabens at locations where a fault is crossing. These sinkholes are comparable to pit craters described by Ferrill et al. (2004, 2011).

Also, during our field work we never observed slickensides at unweathered faulted joint surfaces. Slickenlines should be abundant at discrete slip surfaces in an area with so many faults as the Needles Fault Zone. The absence of such striations indicates dilatant faulting by reactivation of the preexisting joints.

Layers distinctly dipping towards the graben wall require a depression into which they can dip. The GPR profile from Devil's Lane (Fig. 8) shows an example of this situation. At both ends of the profile layers dip towards the respective graben wall. The profile from Devil's Pocket (Fig. 11) partially shows this situation. Layers to the east of fault 1 dip towards the western graben wall and at fault 2 dip occurs from east and west.

## 7.2 Fault shape

The combination of opening of preexisting joints during faulting and the considerable vertical displacement in the grabens requires a change in dip of the faults in depth. The measurements of heave and throw in Devil's Pocket, Devil's Lane and the graben east of Cow Canyon provide direct evidence of fault dip at depth according to geometric considerations illustrated in Fig. 12a. The fault dip  $\alpha$  is defined as  $\alpha = \arctan(\text{throw/heave})$ . Joint surfaces that were once connected are now separated by several meters horizontally while also showing distinct vertical offset. Estimates of this are highly variable and show required fault dips of 60–80° at depth in Devil's Pocket to produce the observed offsets, whereas in other cases very shallow dipping extensional faults are assumed. Disregarding the erosional effect on the heave, in the graben east of Cow Canyon a fault dip of less than 20° is calculated. This can be explained by a secondary low-angle slip on a lubricating layer due to removing the confinement in the initial tensile deformation (see Fig. 12b).

## Evolution of a highly dilatant fault zone in the grabens of Canyonlands National Park

M. Kettermann et al.

Title Page

Abstract

Introduction

Conclusions

References

Tables

Figures

◀

▶

◀

▶

Back

Close

Full Screen / Esc

Printer-friendly Version

Interactive Discussion



## Evolution of a highly dilatant fault zone in the grabens of Canyonlands National Park

M. Kettermann et al.

Title Page

Abstract

Introduction

Conclusions

References

Tables

Figures

◀

▶

◀

▶

Back

Close

Full Screen / Esc

Printer-friendly Version

Interactive Discussion



Other authors found field evidence for such a vertical change of the fault dips in the grabens of the Canyonlands by investigating crosscut grabens along Y Canyon, Cross Canyon and Lower Red Lake Canyon. Based on observations in these crosscuts McGill and Stromquist (1979) proposed that faults are vertical over about 100 m followed by dips of about 75° down to the evaporite interface. This observation was confirmed by Moore and Schultz (1999) by investigations in the same area.

A similar fault geometry is reproduced in the experiments of Holland et al. (2006) and van Gent et al. (2010). They used hemihydrate powder to investigate the evolution of normal faults in brittle materials and observed a tensile fracturing in the upper fault sections, a mixed mode fracture in the middle, and a shallow dipping shear movement in the lowest part of the fault zone. Hence, the surface expression of these faults is a vertical cliff with an open void at the graben-bounding fault and some vertical offset.

This “pull-apart” model in mechanically layered stratigraphy causing opening in the more competent layers is well known from outcrops (e.g. Peacock and Sanderson, 1992; Peacock, 2002; Ferrill and Morris, 2003; Crider and Peacock, 2004; Ferrill et al., 2014) and shown in DEM models as well (e.g. Schöpfer et al., 2007a–c; Abe et al., 2011). We suggest that in the Canyonlands this effect is additionally controlled by the abundant vertical joint sets that are defining the present day graben walls.

Analogue modeling of the interaction of preexisting joints and normal faults in brittle rocks was performed by Kettermann (2012). The basic deformation box, setup and scaling relations were the same as in the work of Holland et al. (2011). Additionally, joints were introduced to the system, by hanging sheets of paper into the box during filling, and carefully removing them before the deformation. As the hemihydrate is cohesive, open joints are formed and can then affect the faulting. The maximum depth of the joints as well as the joint spacing was chosen to represent the situation in the Canyonlands. In a series of experiments the angle between joint strike and fault strike was varied in a range observed in the field. Figure 13 shows a top view of an experiment with 8° angle between joint strike and basement-fault strike. Observed structures are



## Evolution of a highly dilatant fault zone in the grabens of Canyonlands National Park

M. Kettermann et al.

Title Page

Abstract

Introduction

Conclusions

References

Tables

Figures

◀

▶

◀

▶

Back

Close

Full Screen / Esc

Printer-friendly Version

Interactive Discussion



The faults in Devil's Pocket and northern Cyclone Canyon additionally show more than one fault strand. Our observations show that even flat and apparently undisturbed graben floors can contain complex fault systems. As these are not visible at the surface the faults are presumably not active any more.

Combining all the information presented we propose a model for the formation of a typical Canyonlands graben as shown in Fig. 15. Faults dip with 60–80° and intersect the vertical joints. Hence, the outcropping graben walls are joint surfaces rather than fault planes. Inclined faults reactivate the vertical joints at surface, and this change in fault dip forms large open voids at the graben walls, which are then filled with rock fall debris and Quaternary sediments. Additional graben internal faulting causes a complex hard rock topography and requires reactive diapirism of the salt as also suggested by Schultz-Ela and Walsh (2002) and Walsh and Schultz-Ela (2003). As sinkholes are preferably found in the presumably younger grabens in the east and southeast and ponded deposits are observed in the older, western grabens (Cyclone Canyon), this might also be a criterion of graben maturity.

### 7.4 Graben age vs. deposition rates

The GPR profile of central Cyclone Canyon revealed detailed sedimentary structures to a depth of about four meters (Fig. 10). We noticed three distinct horizons of horizontal reflectors and in between delta-like sequences of foreset beds and onlaps. The interpretation of lacustrine delta sediments is supported by typical layering of the dipping sediments, visible by changing reflector intensities, that implies sedimentation in water due to sudden events such as flash-floods. The geological map of Billingsley et al. (2002) shows that ponded deposits are common in Cyclone Canyon and the authors state that these ponds were capable of sustaining water for several months to years. The thickness of the ponded deposits of up to 2 m fits well to the observed thickness in the radar profiles.

Especially the three horizontal layers that we interpret as paleosols fit very well to a graben fill east of Virginia Park, described and dated by Reheis et al. (2005). The

## Evolution of a highly dilatant fault zone in the grabens of Canyonlands National Park

M. Kettermann et al.

Title Page

Abstract

Introduction

Conclusions

References

Tables

Figures

◀

▶

◀

▶

Back

Close

Full Screen / Esc

Printer-friendly Version

Interactive Discussion



location is marked with a black star in Fig. 3b. Thanks to the incision of a stream they were able to visually study a soil-profile down to 6 m depth and apply optically stimulated luminescence (OSL) dating. They described three paleosols, one close to the surface, one in two meters depth, and a third one in about three meters depth.

5 Dating right above the second paleosol results in an age of about 15–16 ka and sediments above the third paleosol were dated to 27–28 ka. Figure 16 shows the GPR profile of the central Cyclone Canyon with the stratigraphic column and OSL-ages of Reheis et al. (2005) as an overlay. The depths of all paleosols match with deviation of only a few cm.

10 Based on the proposed age of the grabens (Biggar and Adams, 1987; Schultz and Moore, 1996; Trudgill, 2002), the sediments thickness in Cyclone Canyon (Grosfils et al., 2003) and the known age of these paleosols (Reheis et al., 2005) we propose three possible scenarios of graben formation and sedimentation:

- 15 1. The horizons in GPR and outcrop are not the same. Still we would interpret the observed horizons as paleosols. Assuming a faster deposition rate in Cyclone Canyon due to its preferred role as a sediment trap would then suggest long-range climate changes within the recorded four meters of the profile and distinct differences in deposition over short distances.
- 20 2. The horizons in GPR and outcrop are the same. An explanation for the small discrepancy in the depth of the paleosols would be a faster sedimentation between the first and second paleosol. This is likely, since Cyclone Canyon is a quite deep graben compared to the one east of Virginia Park and thus a better sediment trap. The delta-like foreset beds observed between the upper two paleosols indicate a high deposition rate in the presence of water, i.e. extensive flash floods as they occur from time to time depositing in ponds. Additionally, slight differences in depth can result from imperfect time-depth conversion. Applying the OSL ages from Reheis et al. (2005) to the depths in Cyclone Canyon allows an estimation of sedimentation rates. Assuming the first OSL age of roughly 16 ka

## SED

7, 1119–1161, 2015

## Evolution of a highly dilatant fault zone in the grabens of Canyonlands National Park

M. Kettermann et al.

Title Page

Abstract

Introduction

Conclusions

References

Tables

Figures

◀

▶

◀

▶

Back

Close

Full Screen / Esc

Printer-friendly Version

Interactive Discussion



in a depth of 2.2 m leads to a sedimentation rate of  $0.14 \text{ mma}^{-1}$  for this section. The distance between the second and third paleosol is approximately the same as in the Virginia Park Graben – one meter – and the age of about 28 ka leads to a sedimentation rate of  $0.08 \text{ mma}^{-1}$ . Seismic refraction data (Abrahamson, 2005) suggest a sediment thickness of about 50 m at this location. Following the suggested ages of graben initiation of 65–85 ka (Campbell, 1987; Schultz and Moore, 1996), the deposition rates below the third paleosol must have been one order of magnitude higher. These would still be reasonable deposition rates, but would suggest a drastic change in the deposition system at one point.

3. In the third case the paleosols are the same, a sediment package of 50 m is given and we assume that the rate of deposition has not changed dramatically in the past. That would point towards an earlier initiation of graben formation than previously estimated by termoluminescence dating of sediments found in sinkholes (Campbell, 1987), although their results may not apply for all grabens. Using a deposition rate of  $0.15 \text{ mma}^{-1}$  as an average for the remaining 47 m beneath our profile results in an age of about 300 ka. This is supported by comparing recent deformation rates with estimates of total strain in the Needles Fault Zone. Westwards movements of  $3\text{--}9 \text{ mma}^{-1}$  were proposed from InSAR data by Furuya et al. (2007). These fit to the GPS data of Marsic (2003), who reported  $5 \text{ mma}^{-1}$ . According to Moore and Schultz (1999) a total extension of 1.29 km took place on the northern section of the grabens. Assuming an average extension of  $5 \text{ mma}^{-1}$  would require an age of graben initiation of about 260 ka, which would fit well to the observed sediment thickness and deposition rates. Schultz-Ela and Walsh (2002) used geomechanical numerical modeling to reproduce the grabens and proposed an age of 135 ka for their models, which is younger than suggested here, but still older than the previous estimates. Grosfils et al. (2003) in contrast calculated a smaller extension of about 2% in Devils Lane and transferred this value to the other grabens, resulting in a total extension of about 100 m and an age fitting to the earlier estimates.

## Evolution of a highly dilatant fault zone in the grabens of Canyonlands National Park

M. Kettermann et al.

Title Page

Abstract

Introduction

Conclusions

References

Tables

Figures

◀

▶

◀

▶

Back

Close

Full Screen / Esc

Printer-friendly Version

Interactive Discussion



To resolve the remaining problems, more data are needed from different grabens and locations. Especially case (1) can only be validated or rejected by drilling in Cyclone Canyon and actually comparing and dating the sediments directly. However, it seems legitimate to assume an intermediate situation of cases (2) and (3). Some authors (Trudgill and Cartwright, 1994; Schultz-Ela and Walsh, 2002) propose graben initiation at 500 ka or more, following the timing of the Colorado River incision. Higher deposition rates are also possible. A mixture of both would be a good explanation for the intermediate age of 260–300 ka proposed in our model.

### 8 Conclusions

By applying ground penetrating radar surveys combined with field observations in the Needles Fault Zone of Canyonlands National Park, Utah/USA, we draw the following conclusions:

1. Our GPR profiles revealed faults in the subsurface that were overprinted and not visible at the surface. We can therefore conclude that the fault zone of the Canyonlands grabens is more complex than obvious. Since this area is an analogue for reservoirs, knowledge of the fault zone complexity can be used to enhance seismic interpretations and fault zone permeability estimates.
2. Dilatant faulting is evident in many places, even if the surface expression is overprinted by sedimentation. Measurements of heave and throw at some faults additionally provide evidence for vertical fractures at the surface in combination with joint reactivation and inclined faults at depth.
3. We propose a model of graben formation based on our observations including fault-joint intersections, shallow fault dips at depth, graben internal faulting and reactive diapirism.

## Evolution of a highly dilatant fault zone in the grabens of Canyonlands National Park

M. Kettermann et al.

Title Page

Abstract

Introduction

Conclusions

References

Tables

Figures

◀

▶

◀

▶

Back

Close

Full Screen / Esc

Printer-friendly Version

Interactive Discussion

4. Paleosols in the subsurface of Cyclone Canyon correlate with the climate reconstruction of Reheis et al. (2005). Comparing these paleosols, their ages and the underlying sediment thicknesses imply either a graben age older than expected from previous dating or higher sedimentation rates in Cyclone Canyon.

5 **The Supplement related to this article is available online at doi:10.5194/sed-7-1119-2015-supplement.**

*Acknowledgements.* We like to thank Marc Miller and Vicky Webster from the National Park Service for their kind support in the preparation of the field study.

### References

- 10 Abe, S., van Gent, H., and Urai, J. L.: DEM simulation of normal faults in cohesive materials, *Tectonophysics*, 512, 12–21, 2011.
- Abrahamson, J.: Determining the thickness of sediments using seismic refraction, Cyclone Canyon Graben, Canyonlands National Park, Utah, in: 18th Annual Keck Research Symposium in Geology 2005, Colorado Springs, Colorado, USA, 7–10, 2005.
- 15 Angelier, J., Bergerat, F., Dauteuil, O., and Villemin, T.: Effective tension–shear relationships in extensional fissure swarms, axial rift zone of northeastern Iceland, *J. Struct. Geol.*, 19, 673–685, 1997.
- Baker, A. A.: *Geology and Oil Possibilities of the Moab District, Grand and San Juan Counties, Utah*, US Geological Survey Bulletin 841, Washington, D.C., 1933.
- 20 Biggar, N. E. and Adams, J. A.: Dates derived from Quaternary strata in the vicinity of Canyonlands National Park, in: *Geology of Cataract Canyon and Vicinity: A Field Symposium – Guidebook of the Four Corners Geological Society*, edited by: Campbell, J. A., Canyonlands Research Bibliography, Paper No. 327, 127–136, 1987.
- Billingsley, G. H., Block, D. L., and Felger, T. J.: *Surficial Geologic Map of The Loop and Druid Arch Quadrangles, Canyonlands National Park, Utah*, WWW document, available at: <http://>
- 25



## Evolution of a highly dilatant fault zone in the grabens of Canyonlands National Park

M. Kettermann et al.

Title Page

Abstract

Introduction

Conclusions

References

Tables

Figures

◀

▶

◀

▶

Back

Close

Full Screen / Esc

Printer-friendly Version

Interactive Discussion

implications for hydrocarbon migration and accumulation, AAPG Bulletin, 94, 597–613, 2010.

Furuya, M., Mueller, K., and Wahr, J.: Active salt tectonics in the Needles District, Canyonlands (Utah) as detected by interferometric synthetic aperture radar and point target analysis: 1992–2002, *J. Geophys. Res.*, 112, B06418, doi:10.1029/2006JB004302, 2007.

Golstrand, P. M.: Tectonic development of Upper Cretaceous to Eocene strata of southwestern Utah, *Geol. Soc. Am. Bull.*, 106, 145–154, 1994.

Grosfils, E. B., Schultz, R. A., and Kroeger, G.: Geophysical exploration within northern Devils Lane Graben, Canyonlands National Park, Utah: implications for sediment thickness and tectonic evolution, *J. Struct. Geol.*, 25, 455–467, 2003.

Gudmundsson, A. and Bäckström, K.: Structure and development of the Sveinagja Graben, Northeast Iceland, *Tectonophysics*, 200, 111–125, 1991.

Gutiérrez, F.: Origin of the salt valleys in the Canyonlands section of the Colorado Plateau, *Geomorphology*, 57, 423–435, 2004.

Hintze, L. F., Willis, G. C., Laes, D. Y. M., Sprinkel, D. A., and Brown, K. D.: Digital Geological Map of Utah, Utah Geological Survey in cooperation with the USGS, Salt Lake City, Utah, USA, 2000.

Holland, M., Urai, J. L., and Martel, S.: The internal structure of fault zones in basaltic sequences, *Earth Planet. Sc. Lett.*, 248, 301–315, 2006.

Holland, M., van Gent, H., Bazalgette, L., Yassir, N., Hoogerduijn Strating, E. H., and Urai, J. L.: Evolution of dilatant fracture networks in a normal fault – evidence from 4-D model experiments, *Earth Planet. Sc. Lett.*, 304, 399–406, 2011.

Huntoon, P. W.: The Meander Anticline, Canyonlands, Utah: an unloading structure resulting from horizontal gliding on salt, *Geol. Soc. Am. Bull.*, 93, 941–950, 1982.

Huntoon, P. W., Billingsley, G. H., and Breed, W. J.: Geologic Map of Canyonlands National Park and Vicinity, Canyonlands National History Assoc., Moab, Utah, 1982.

Jafari, A. and Babadagli, T.: Effective fracture network permeability of geothermal reservoirs, *Geothermics*, 40, 25–38, 2011.

Kettermann, M.: The Effect of Preexisting Joints on Normal Fault Evolution – Insights from Fieldwork and Analogue Modeling, M.Sc. thesis, RWTH Aachen University, Aachen, Germany, 2012.





## Evolution of a highly dilatant fault zone in the grabens of Canyonlands National Park

M. Kettermann et al.

Title Page

Abstract

Introduction

Conclusions

References

Tables

Figures

◀

▶

◀

▶

Back

Close

Full Screen / Esc

Printer-friendly Version

Interactive Discussion



Trudgill, B. and Cartwright, J.: Relay-ramp forms and normal-fault linkages, Canyonlands National Park, Utah, *Geol. Soc. Am. Bull.*, 106, 1143–1157, 1994.

Utah Automated Geographic Reference Center: HRO 1-Foot Color Orthophotography, WWW document, available at: <http://gis.utah.gov/data/aerial-photography/2009-hro-1-foot-color-orthophotography/>, last access: 12 March 2015, 2009.

Van Gent, H. W., Holland, M., Urai, J. L., and Loosveld, R.: Evolution of fault zones in carbonates with mechanical stratigraphy – insights from scale models using layered cohesive powder, *J. Struct. Geol.*, 32, 1375–1391, 2010.

Van Heteren, S., Fitzgerald, D. M., Mckinlay, P. A., and Buynevich, I. V.: Radar facies of paraglacial barrier systems: coastal New England, USA, *Sedimentology*, 45, 181–200, 1998.

Walsh, J., Bailey, W., Childs, C., Nicol, A., and Bonson, C.: Formation of segmented normal faults: a 3-D perspective, *J. Struct. Geol.*, 25, 1251–1262, 2003.

Walsh, J. J., Watterson, J., Bailey, W. R., and Childs, C.: Fault relays, bends and branch-lines, *J. Struct. Geol.*, 21, 1019–1026, 1999.

Walsh, P. and Schultz-Ela, D. D.: Mechanics of graben evolution in Canyonlands National Park, Utah, *Geol. Soc. Am. Bull.*, 115, 259–270, 2003.

Wennberg, O. P., Malm, O., Needham, T., Edwards, E., Ottesen, S., Karlsten, F., Rennan, L., and Knipe, R.: On the occurrence and formation of open fractures in the Jurassic reservoir sandstones of the Snohvit Field, SW Barents Sea, *Petrol. Geosci.*, 14, 139–150, 2008.

Wilkins, S. J. and Gross, M. R.: Normal fault growth in layered rocks at Split Mountain, Utah: influence of mechanical stratigraphy on dip linkage, fault restriction and fault scaling, *J. Struct. Geol.*, 24, 1413–1429, 2002.

Wong, I. G., Olig, S. S., and Bott, J. D. J.: Earthquake Potential and Seismic Hazards in the Paradox Basin, Southeastern Utah, *Geology and Resources of the Paradox Basin, Utah Geological Association Guidebook 25*, Salt Lake City, Utah, USA, 241–251, 1993.

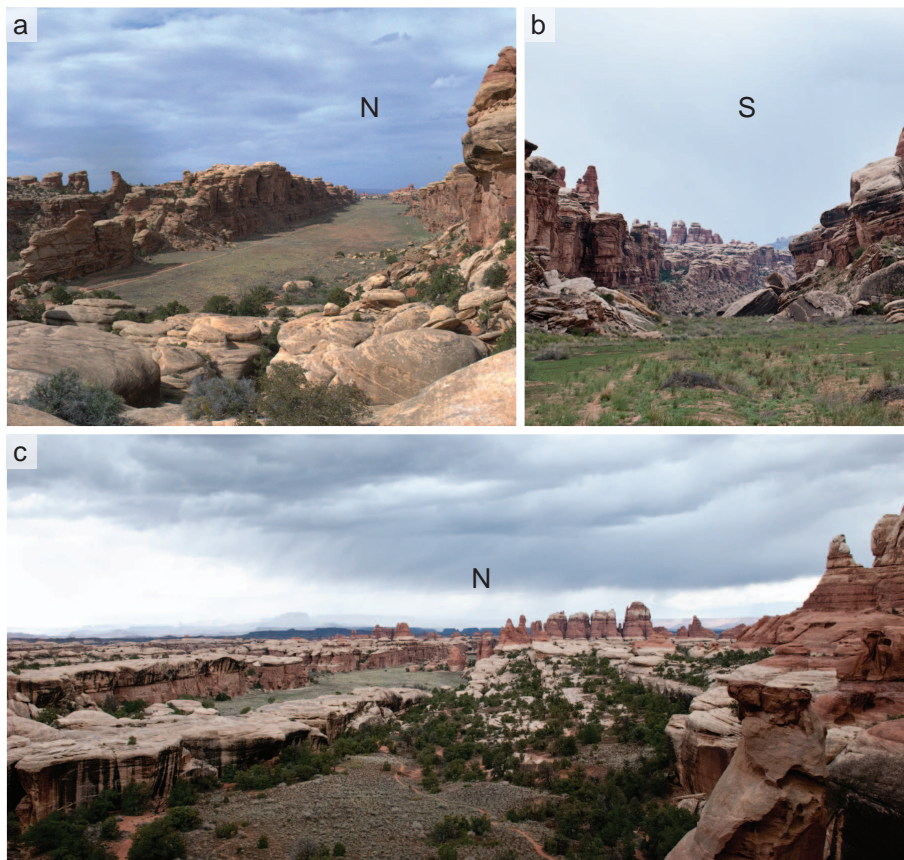


**Figure 1.** (a) Field photograph from the Devil's Lane relay facing north. (b) Northern Cyclone Canyon looking south. (c) View over the southern part of Devil's Pocket looking north.

**Evolution of a highly dilatant fault zone in the grabens of Canyonlands National Park**

M. Kettermann et al.

Title Page

Abstract

Introduction

Conclusions

References

Tables

Figures

◀

▶

◀

▶

Back

Close

Full Screen / Esc

Printer-friendly Version

Interactive Discussion



# SED

7, 1119–1161, 2015

## Evolution of a highly dilatant fault zone in the grabens of Canyonlands National Park

M. Kettermann et al.

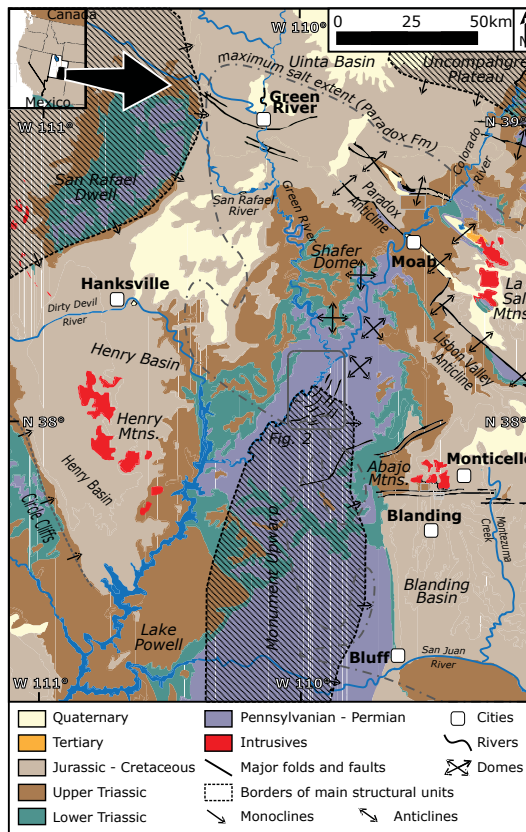


**Figure 2.** Geology of SE Utah and major structural units. Inlet indicates location of Fig. 3. Study area (grabens in the Canyonland National Park) is located at northern end of the Monument Upward, east of the Colorado River. Geological and structural data compiled from Huntoon et al. (1982), Condon (1997), Hintze et al. (2000), Gutiérrez (2004).

Title Page

Abstract Introduction

Conclusions References

Tables Figures

◀ ▶

◀ ▶

Back Close

Full Screen / Esc

Printer-friendly Version

Interactive Discussion

## Evolution of a highly dilatant fault zone in the grabens of Canyonlands National Park

M. Kettermann et al.

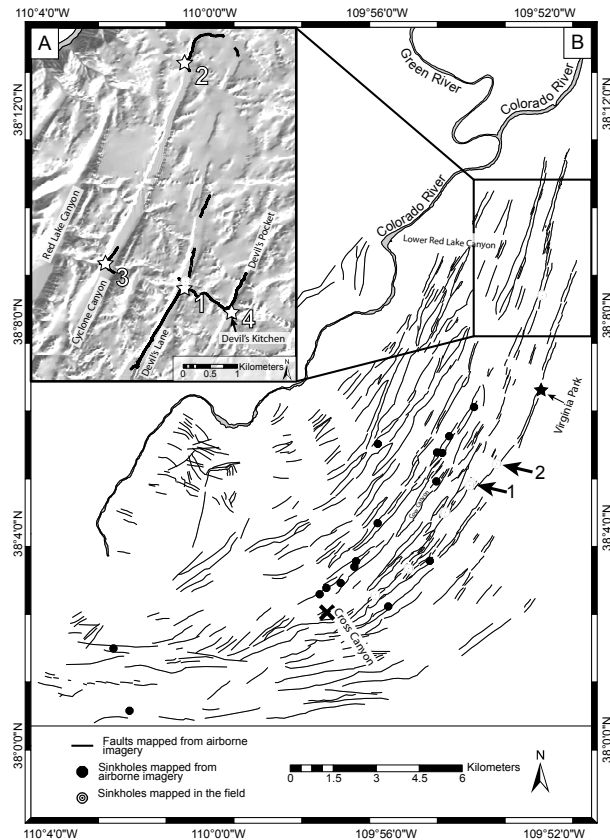


**Figure 3.** (a) Needles Area, northern part of the Grabens as a hillshade digital elevation model (National Elevation Dataset, NED). Presented GPR profiles indicated by numbered stars. Entire collected GPR dataset is shown by black lines. (b) Overview of the Canyonlands grabens. Graben-bounding faults mapped via orthoimagery. Sinkholes mapped in the field and from imagery.

Title Page

Abstract

Introduction

Conclusions

References

Tables

Figures

◀

▶

◀

▶

Back

Close

Full Screen / Esc

Printer-friendly Version

Interactive Discussion

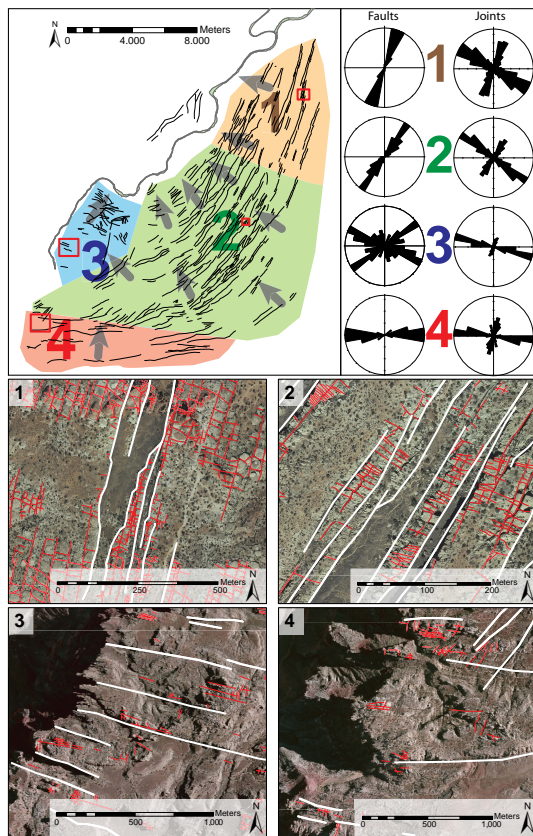


**Figure 4.** Fault and joint orientations in the Needles Fault Zone derived from airborne image mapping. Four sections group areas of similar orientations. One joint set is always parallel to the major faults. Small red rectangles depict locations of associated detail photographs showing the interpretations of faults (white lines) and joints (red lines). Numbers 1–4 on the photographs correspond to the sections.

Evolution of a highly dilatant fault zone in the grabens of Canyonlands National Park

M. Kettermann et al.

Title Page

Abstract Introduction

Conclusions References

Tables Figures

◀ ▶

◀ ▶

Back Close

Full Screen / Esc

Printer-friendly Version

Interactive Discussion



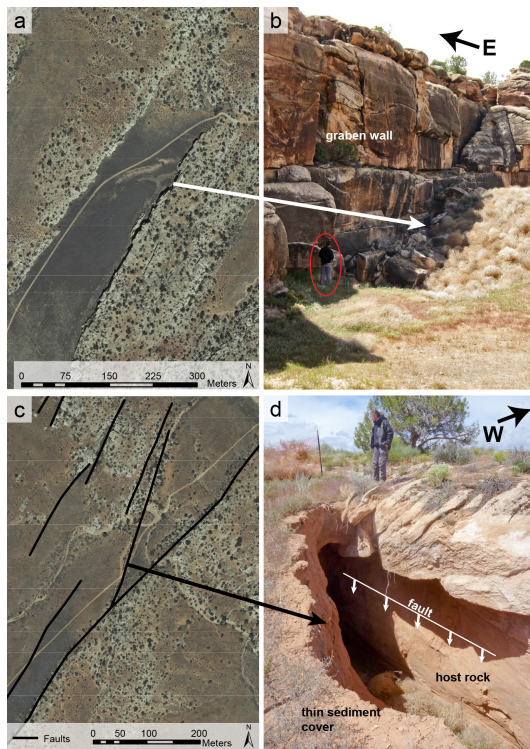


**Figure 5.** (a) Aerial photograph showing the location and surface depression of a large sinkhole (cf. arrow “1” in Fig. 3). (b) Field photograph shows the same sinkhole (person in the ellipse for scale). Material is lost into a cavity or an interconnected system of open fractures allowing an outflow of sediments in the subsurface. (c) Airborne photograph shows location of another sinkhole not located at a graben wall (cf. arrow “2” in Fig. 3) but at a graben crossing fault. (d) Corresponding field photograph illustrating open gap at fault.

**Evolution of a highly dilatant fault zone in the grabens of Canyonlands National Park**

M. Kettermann et al.

Title Page	
Abstract	Introduction
Conclusions	References
Tables	Figures
◀	▶
◀	▶
Back	Close
Full Screen / Esc	
Printer-friendly Version	
Interactive Discussion	

## Evolution of a highly dilatant fault zone in the grabens of Canyonlands National Park

M. Kettermann et al.

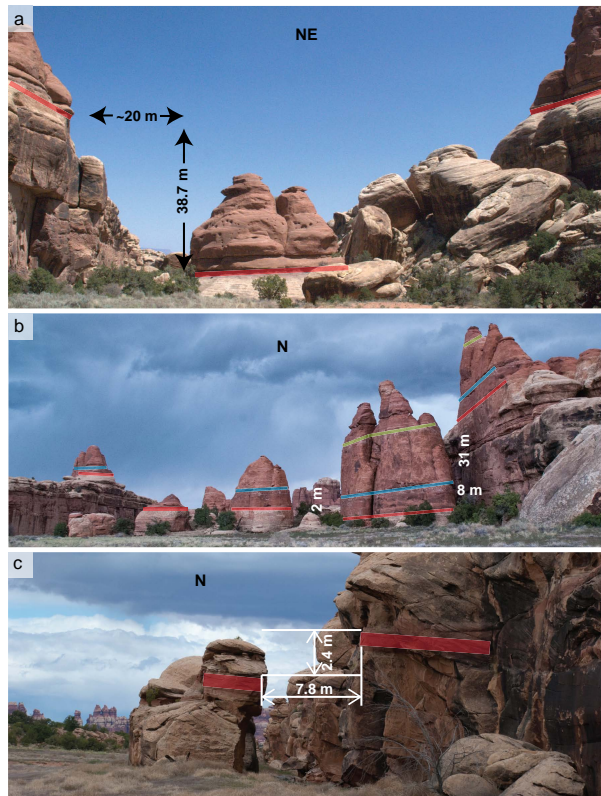


**Figure 6.** Three locations where heave and throw were measured and fault-dips at depth were estimated. **(a)** Northern Devil's Pocket. **(b)** Southern Devil's Pocket. **(c)** Unnamed graben east of Cow Canyon. Individual heave and throw values are given in images.

Title Page

Abstract

Introduction

Conclusions

References

Tables

Figures

◀

▶

◀

▶

Back

Close

Full Screen / Esc

Printer-friendly Version

Interactive Discussion

## Evolution of a highly dilatant fault zone in the grabens of Canyonlands National Park

M. Kettermann et al.

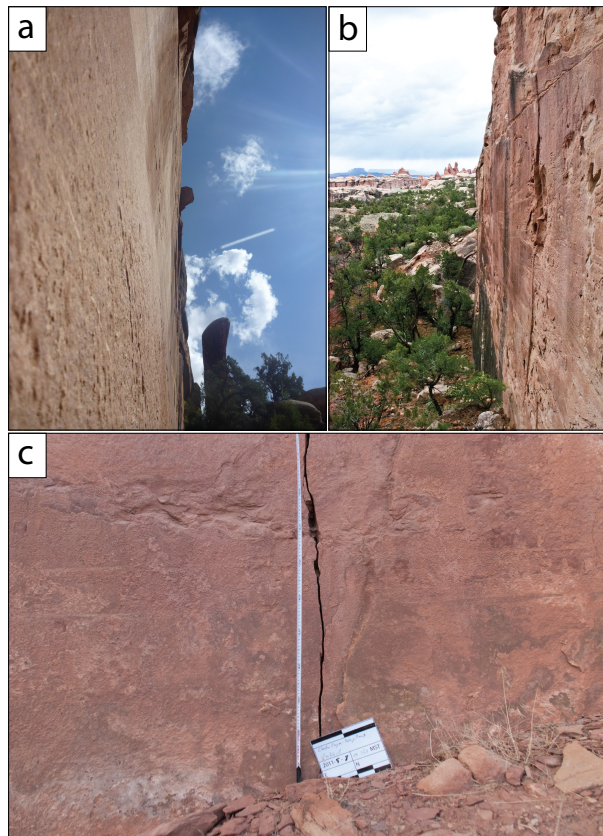


**Figure 7.** Unweathered joint surfaces at faults showing no slickenlines or toolmarks **(a)** northern Devil's Pocket, **(b)** southern end of Devil's Pocket, **(c)** Devil's Lane relay.

Title Page

Abstract

Introduction

Conclusions

References

Tables

Figures

◀

▶

◀

▶

Back

Close

Full Screen / Esc

Printer-friendly Version

Interactive Discussion

## Evolution of a highly dilatant fault zone in the grabens of the Canyonlands National Park

M. Kettermann et al.

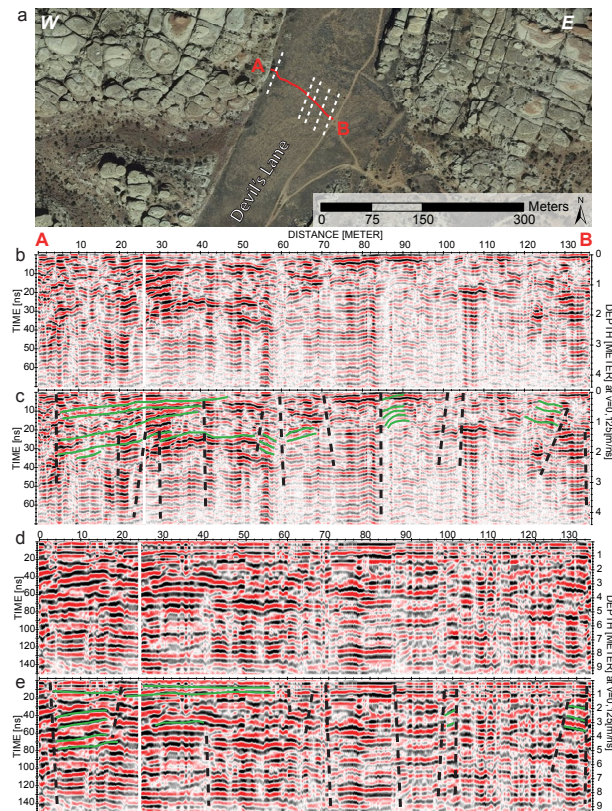


**Figure 8.** WNW–ESE profiles crossing through Devil's Lane. **(a)** Aerial photograph of the profile (red line). Interpreted faults are indicated by white dashed lines. **(b and d)**: 400 and 100 MHz profiles without interpretation. **(c and e)**: 400 and 100 MHz profiles with interpretation (green lines: interpreted layers, dashed line: interpreted faults).

## Evolution of a highly dilatant fault zone in the grabens of Canyonlands National Park

M. Kettermann et al.

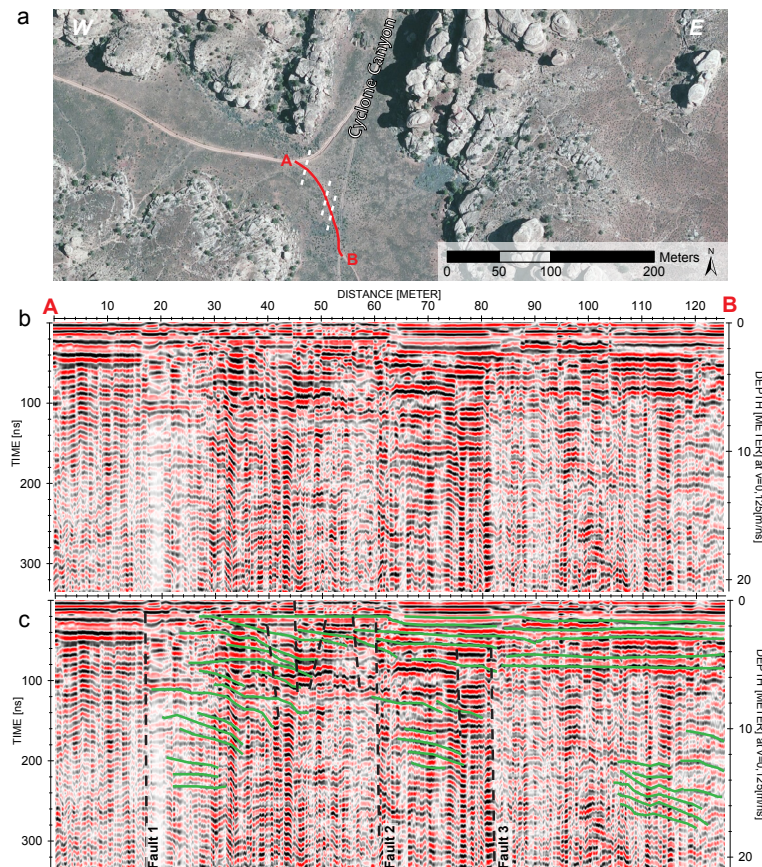


**Figure 9.** NW–SE profile in northern Cyclone Canyon. **(a)** Airborne image illustrating pathway of the profile. **(b)** 100 MHz profile without interpretation. **(c)** Profile with interpretation (green lines: interpreted layers, dashed line: interpreted faults).

## Evolution of a highly dilatant fault zone in the grabens of Canyonlands National Park

M. Kettermann et al.

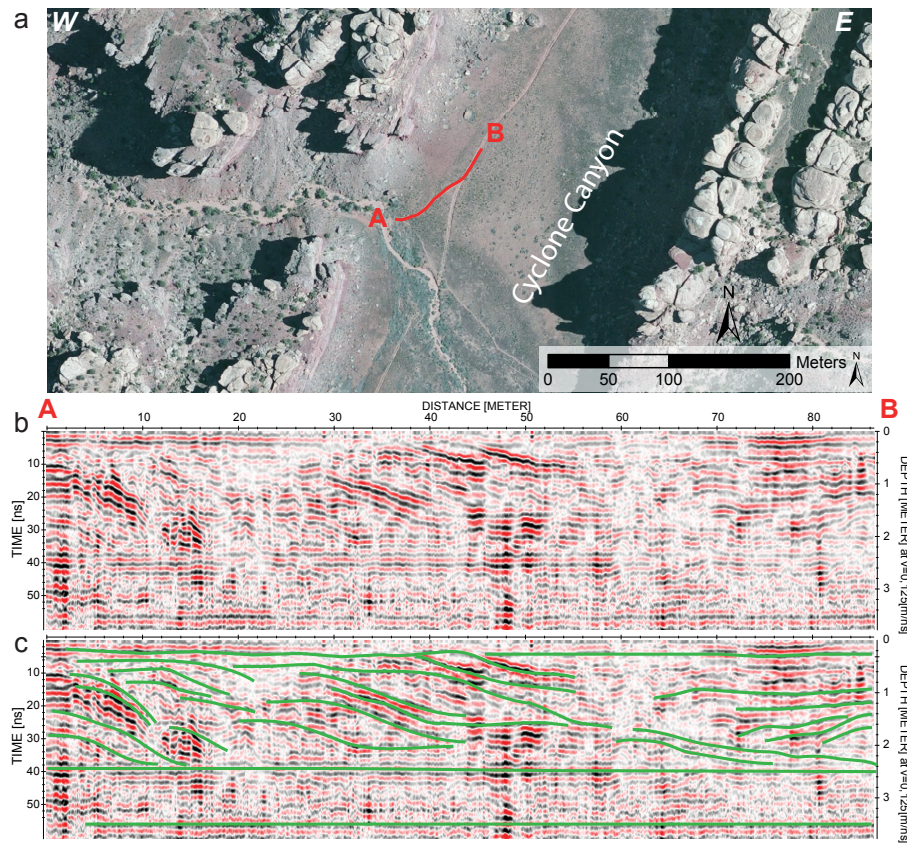


**Figure 10.** SW–NE profile crossing the central Cyclone Canyon. **(a)** Aerial photograph illustrating the trace of the profile (red line). **(b)** 400 MHz Profile without interpretation. **(c)** Profile with interpretation (green lines: interpreted layers, dashed line: interpreted faults).

## Evolution of a highly dilatant fault zone in the grabens of Canyonlands National Park

M. Kettermann et al.

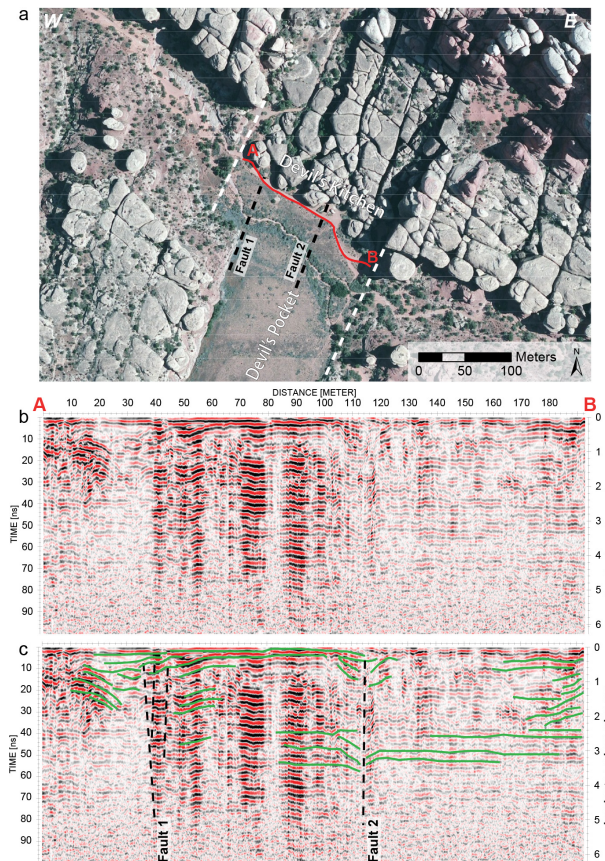


**Figure 11.** Devil's Kitchen WNW–ESE profile. **(a)** Aerial photograph showing location of the profile, interpreted faults (black lines) and known graben bounding faults (white lines). **(b)** 400 MHz profile without interpretation. **(c)** Profile with interpretation (green lines: interpreted layers, dashed line: interpreted faults).

## Evolution of a highly dilatant fault zone in the grabens of Canyonlands National Park

M. Kettermann et al.

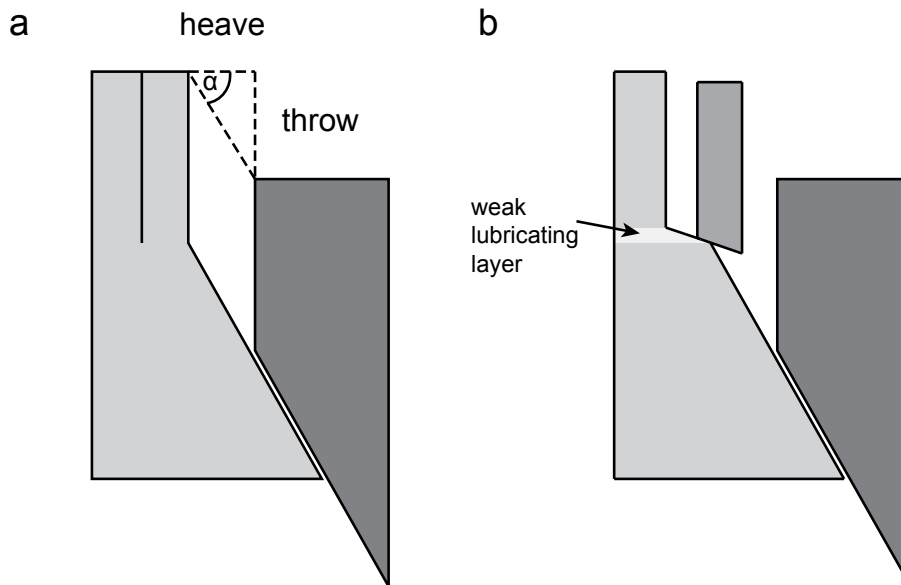


**Figure 12.** (a) Geometric relation between heave, throw and fault dip. (b) Lubricating layer can cause large blocks to break down.

Title Page

Abstract

Introduction

Conclusions

References

Tables

Figures

◀

▶

◀

▶

Back

Close

Full Screen / Esc

Printer-friendly Version

Interactive Discussion



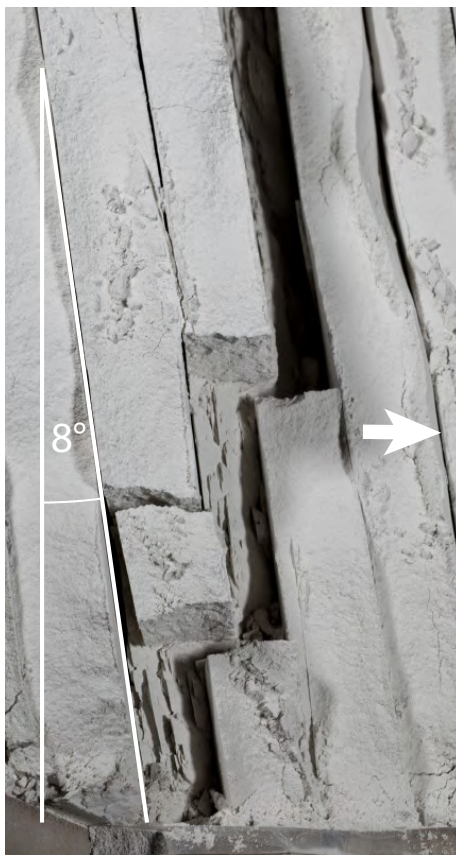


**Figure 13.** Top view image showing an analogue experiment of Kettermann (2012) with  $8^\circ$  fault-joint angle after deformation. Main fault localized at preexisting joints exclusively; open gaps formed where the shallower dipping fault cuts the vertical joints. Original joint surfaces are preserved.

**Evolution of a highly dilatant fault zone in the grabens of Canyonlands National Park**

M. Kettermann et al.

Title Page

Abstract

Introduction

Conclusions

References

Tables

Figures

◀

▶

◀

▶

Back

Close

Full Screen / Esc

Printer-friendly Version

Interactive Discussion

## Evolution of a highly dilatant fault zone in the grabens of Canyonlands National Park

M. Kettermann et al.

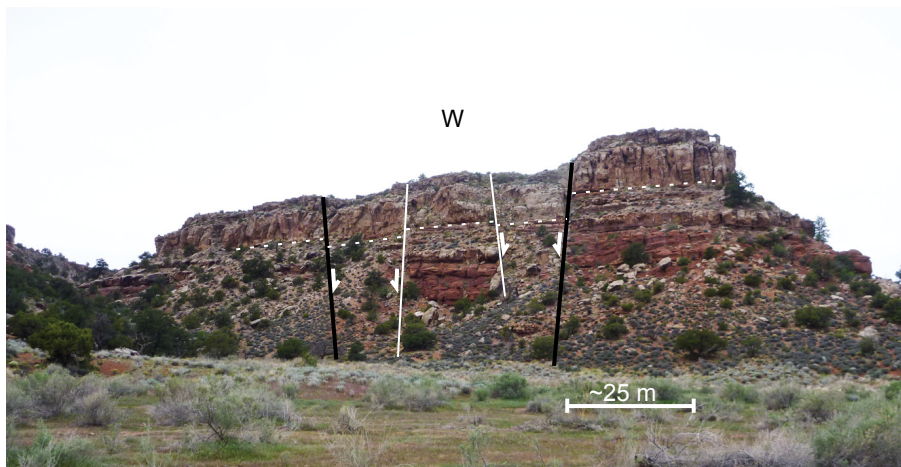


**Figure 14.** Graben in Cross Canyon. Black lines show main graben bounding faults. White lines show two conjugate faults cutting through the graben floor. Dashed line illustrates marker horizon. Example for intra-graben faulting.

Title Page

Abstract

Introduction

Conclusions

References

Tables

Figures

◀

▶

◀

▶

Back

Close

Full Screen / Esc

Printer-friendly Version

Interactive Discussion

# SED

7, 1119–1161, 2015

## Evolution of a highly dilatant fault zone in the grabens of Canyonlands National Park

M. Kettermann et al.

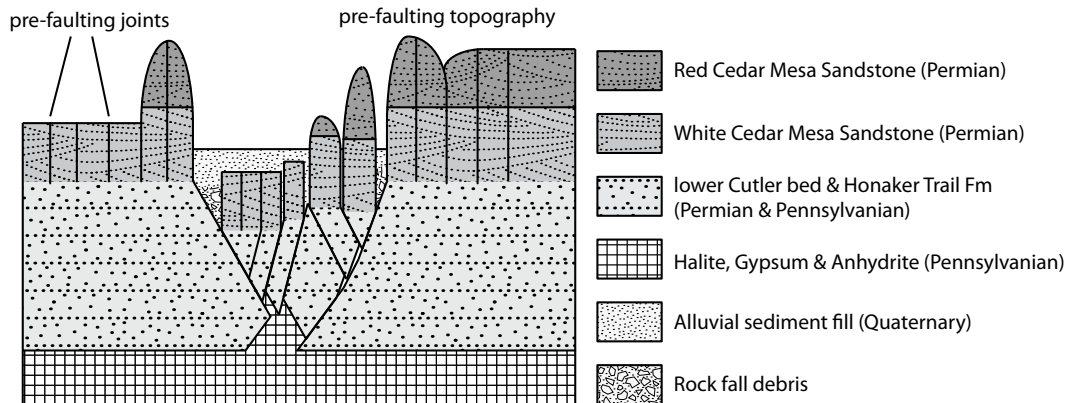


**Figure 15.** Schematic model of a typical Canyonlands graben from the northern section. Joints of the Cedar Mesa sandstones are reactivated by faulting. Shallower fault dips at depth causes open gaps at surface and secondary faulting within the grabens. Rock fall debris and Quaternary alluvial sediments fill up open gaps and graben floors.

## Evolution of a highly dilatant fault zone in the grabens of Canyonlands National Park

M. Kettermann et al.

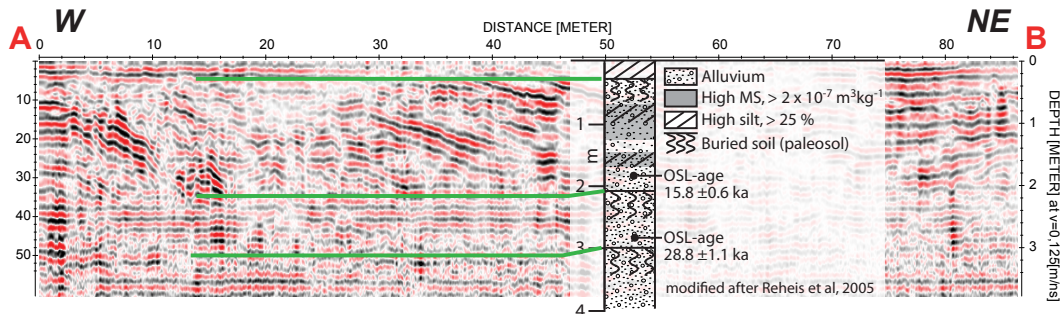


**Figure 16.** 400 MHz profile of central Cyclone Canyon with overlay of the profile and OSL-ages of Reheis et al. (2005). Three horizontal layers in the GPR profile fit well to paleosols from outcrop profile with an error of less than 0.5 m.

Title Page

Abstract

Introduction

Conclusions

References

Tables

Figures

◀

▶

◀

▶

Back

Close

Full Screen / Esc

Printer-friendly Version

Interactive Discussion